Biochemistry

Article

pubs.acs.org/biochemistry

# Reconstructed Serine 288 in the Left Flipper Region of the Rat P2X7 Receptor Stabilizes Nonsensitized States

Yevheniia Ishchenko,[†] Nataliia Novosolova,[†] Kamil Khafizov,[‡,§] Geneviève Bart,[†,⊥] Arina Timonina,[†] Dmitriy Fayuk,[†] Andrei Skorinkin,[∥,#] and Rashid Giniatullin*[,†,@]

[†]A. I. Virtanen Institute, University of Eastern Finland, Kuopio, Finland

[‡]Moscow Institute of Physics and Technology, Dolgoprudny, Moscow Region, Russian Federation

[§]Central Research Institute of Epidemiology, Moscow, Russian Federation

[∥]Department of Biophysics of Synaptic Processes, Kazan Institute of Biochemistry and Biophysics, Russian Academy of Sciences, Kazan, Russian Federation

[⊥]Faculty of Biochemistry and Molecular Medicine, University of Oulu, Oulu, Finland

[#]Lab of Neuropharmacology, Kazan Federal University, Kazan, Russian Federation

[@]Lab of Neurobiology, Kazan Federal University, Kazan, Russian Federation

**ABSTRACT:** Serine 275, a conserved residue of the left flipper region of ATP-gated P2X3 receptors, plays a key role in both agonist binding and receptor desensitization. It is conserved in most of the P2X receptors except P2X7 and P2X6. By combining experimental patch-clamp and modeling approaches, we explored the role of the corresponding residue in the rat P2X7 receptor (rP2X7) by replacing the phenylalanine at position 288 with serine and characterizing the membrane currents generated by either the wild-type (WT) or the mutated rP2X7 receptor. F288S, an rP2X7 mutation, slowed the deactivation subsequent to 2 and 20 s applications of 1 mM ATP. F288S also prevented sensitization (a progressive current growth) observed with the WT in response to a 20 s application of 1 mM ATP. Increasing the ATP concentration to 5 mM promoted sensitization also in the mutated rP2X7 receptor, accelerating the deactivation rate to typical WT values. YO-PRO1 uptake in cells expressing either the WT or the F288S P2X7 receptor was consistent with recorded membrane current data. Interestingly, in the human P2X7 (hP2X7) receptor, substitution Y288S did not change the deactivation rate, while the Y288F mutant generated a "rat-like" phenotype with a fast deactivation rate. Our combined experimental, kinetic, and molecular modeling data suggest that the rat F288S novel phenotype is due to a slower rate of ATP binding and/or unbinding and stabilization of nonsensitized receptor states.

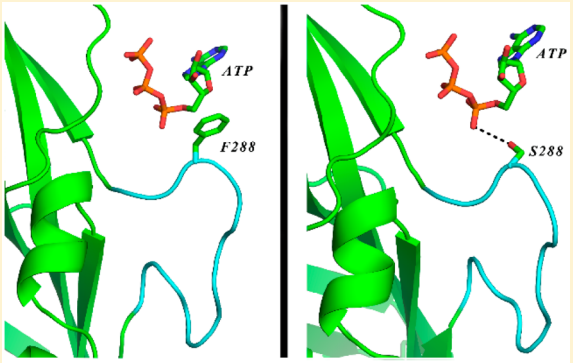




Trimeric P2X receptors, which are composed of P2X1−7 subunits, make up a family of ligand-gated receptors activated by extracellular ATP.[1] A number of crystal structures of P2X receptors have been published over the past several years, greatly extending our understanding of their structure and function. The first structure of the zebrafish P2X4 receptor in the closed state[2] provided extremely valuable information, also opening the possibility of structural modeling of other types of P2X receptors, which resulted in a number of publications.[3,4] More recently, new X-ray models of the zebrafish P2X4 receptor in both the ATP-bound open and closed states were reported,[5] further improving our knowledge of how the structural changes occur upon agonist binding and receptor activation. Finally, structures of hP2X3, giant panda P2X7 (pP2X7), tick P2X, and zebrafish P2X4 (zfP2X4) receptors were published[6−9] in the various states and in the presence of different ligands, including ATP and its analogues, basically giving a detailed picture of most of the structural changes happening during the receptor functional cycle. However, one of the main and still largely unknown issues is identifying subunit-specific functional properties of P2X receptors underlying fundamental phenomena such as desensitization and sensitization.[10−12]

A specific region in the ectodomain of P2X receptors called the "left flipper"[2] faces the ATP binding pocket and was the subject of several recent investigations.[13−16] We previously reported that the conserved serine 275 in the left flipper region plays an essential role in the function of ATP-gated P2X3 receptors.[13] In particular, we proposed that this residue contributes to agonist binding and to receptor desensitization. This role of S275 in agonist binding was indeed recently

**Received:** March 21, 2017
**Revised:** June 14, 2017
**Published:** June 15, 2017




DOI: 10.1021/acs.biochem.7b00258
*Biochemistry* 2017, 56, 3394−3402

confirmed with a new structure of the P2X3 receptor in the ATP-bound state.[7]

The P2X7 subtype (and to a lesser extent the P2X2 and P2X4 subtypes), in addition to the opening of the typical nonselective cationic channel during short agonist applications, can also open a large ion pore during more prolonged applications.[17,18] P2X7 receptors are mainly expressed in immune and glial cells.[19,20] Activation of P2X7 receptors by extracellular ATP promotes the release of cytokines, including IL-1$\beta$,[21−25] and represents an attractive target for the development of anti-inflammatory drugs. In addition, it was discovered that there is a connection between the ATP binding "left flipper" and the pore-lining transmembrane helix through the turret, which supports movements of the upper body domain and tightly coordinates with channel opening in the P2X7 receptor. In contrast to channel opening of P2X3 and P2X4, additional unique conformational changes occur during P2X7 channel opening: both the "left flipper" and the turret narrow with ATP binding.[6]

A kinetic model of the P2X7 receptor activated by its specific agonist BzATP was recently published, presenting a mechanistic explanation for two concurrent processes: desensitization and sensitization.[26] Desensitization, known as "a reversible reduction in response during sustained agonist application",[27] quickly develops at high agonist concentrations,[28] whereas sensitization is a phenomenon associated with generation of the secondary peak (also interpreted as a pore dilation). The nature and the probability of pore dilation are currently subjects of ongoing discussion triggered by the recent studies of Li et al.[29] and Harkat et al.[30] These authors suggested an alternative explanation for secondary peak generation, including an ion depletion mechanism. Therefore, we used the term "sensitization" that formally describes the progressive growth of the current during ATP application[26] in a manner independent of its mechanism. Thus, we operated with a "desensitized" receptor state and with a "sensitized" state, in contrast to the "normal" receptor opening that we here call "nonsensitized".

The amino acid residue at position 288 (P2X7 numbering) is found to be serine in all mammalian P2X receptors except the P2X6 and P2X7 subtypes. In the study presented here, to explore the general role of residues in the left flipper of P2X receptors and the specific role of residue 288, we made a point mutation to add serine instead of phenylalanine at position 288 of the rat P2X7 subtype and using a multidisciplinary approach explored the functional properties of the mutant. We further compared the hP2X7 wild type (WT) with mutants Y288S and Y288F and found that the latter shows rat-like deactivation kinetics. Our approach included the kinetic model of Khadra et al.[26] that we further developed to simulate the P2X7 receptor activated by its natural agonist, ATP. In addition to the uncovered functional role of F288 in the WT rat P2X7 receptor, our combined approach also helped us to explore the basic properties of nonsensitized, desensitized, and sensitized rat P2X7 receptor states.

## EXPERIMENTAL PROCEDURES

**Electrophysiology.** Human embryonic kidney (HEK293) cells were prepared and transfected as previously reported.[13] Transfected cells were plated on coverslips coated in poly-L-lysine (0.2 mg/mL) and cultured for 1−3 days at 37 °C in an atmosphere containing 5% $CO_2$. Transmembrane currents were recorded in the whole cell configuration using the HEKA PC-10 amplifier (HEKA Elektronik) and patch pipettes with a resistance of 4−6 MΩ when filled with 130 mM CsCl, 10 mM HEPES, 5 mM EGTA, 0.5 mM $CaCl_2$, 5 mM $MgCl_2$, 5 mM K-ATP, and 0.5 mM Na-GTP (pH adjusted to 7.2 with CsOH) with an osmolarity of ∼300 mOsm. During experiments, cells were continuously perfused (3 mL/min) with a physiological solution containing 152 mM NaCl, 5 mM KCl, 1 mM $MgCl_2$, 2 mM $CaCl_2$, 10 mM glucose, and 10 mM HEPES (pH adjusted to 7.4 with NaOH). Currents were recorded from cells voltage clamped at −70 mV. Both agonists (Sigma-Aldrich), ATP (pH adjusted to 7.4) and BzATP, were applied via a rapid (exchange time of ∼20 ms) superfusion system (RSC-200, BioLogic, Grenoble, France). To avoid receptor facilitation and to minimize receptor desensitization and sensitization, we used 6−10 min intervals between ATP applications or used naïve receptors for dose−response construction (or an interval increased to 30 min). Recorded data were analyzed using Origin version 8.0 (Microcal, Northampton, MA) and FitMaster (HEKA Elektronik). $EC_{50}$ values were calculated after the fitting of the dose−response curve by the Hill equation.

**Kinetic Modeling.** We used a computer simulation method for the description of WT or F288S kinetics. The modeling is based on solving ordinary differential equations, composed on the basis of mass action law. To compose the equations, we used a previously published kinetic model of the P2X7 receptor activated by the agonist BzATP,[26] which assumed binding of three agonist molecules and a bicycle mode of operation. Four open states were presented in the model: two nonsensitized (with two and three associated ATP molecules) and two sensitized (with two and three associated ATP molecules). Sensitized open states have conductance values that are 3 times higher than that of the nonsensitized open state.[26] The full structure of the model and respective rate constants are shown in Figure 3. The program was written in Pascal to solve numerically the set of differential equations using the eight-order Runge−Kutta method. This program allows calculation of the probabilities of existence of every receptor state (12 states in total as shown in Figure 3).

Transmembrane current $I(t)$ under voltage clamp conditions can be calculated by the following equation:

$$I(t) = N\sigma(V - V_{eq})P_{open}(t) \quad (1)$$

where $V$ is the membrane potential, $V_{eq}$ is the equilibrium potential, $N$ is the total quantity of channels in the membrane, $P_{open}(t)$ is the probability of all open states at time $t$, and $\sigma$ is the single-channel conductance. As it is not possible to control the number of channels in the membrane ($N$), we did not compare current amplitudes, but if $V$, $V_{eq}$, $N$, and $\sigma$ are constants (as we suggested), then the current is proportional to the number of open channels. In this case, the shape of the transmembrane current in all conditions can be found by $P_{open}(t)$ analysis. $P_{open}(t)$ can be calculated by the equation

$$P_{open}(t) = P_{A_2R}(t) + P_{A_3R}(t) + 3[P_{A_2S}(t) + P_{A_3S}(t)] \quad (2)$$

where $P_{A_2R}(t)$, $P_{A_3R}(t)$, $P_{A_2S}(t)$, and $P_{A_3S}(t)$ are the probabilities of double-bound nonsensitized, triple-bound nonsensitized, double-bound sensitized, and triple-bound sensitized open states, respectively. This model also allows the analysis of the contribution of sensitized and nonsensitized states to the total current.

**Molecular Modeling.** The homology models of P2X7 WT and F288S mutant receptors were constructed using the crystal



DOI: 10.1021/acs.biochem.7b00258
Biochemistry 2017, 56, 3394−3402

structure of the ATP-bound state of the P2X7 receptor from giant panda as a template[6] and Modeler 9v12.[31] The ATP molecule present in the binding pocket was retained in the same position. No extra constraints were introduced during the modeling procedure. Alignment of the two amino acid sequences (pP2X7 and rP2X7) was performed using AlignMe;[32] 100 models were constructed, but only a single one was chosen for further analysis on the basis of the lowest molpdf value. Pymol (The PyMOL Molecular Graphics System, version 1.2r3pre, Schrödinger, LLC) was used to visualize three-dimensional models.

**Sequence Analysis.** Amino acid sequences of P2X receptors were obtained from the NCBI database, and multiple-sequence alignments were constructed using Muscle.[33] Jalview[34] was used to visualize the alignments.

**FACS with YO-PRO1.** Fluorescent dye uptake by P2X7 receptors was studied using FACS as first described in ref 35 with small modifications. Briefly, HEK293 cells were transfected with rat P2X7 WT and F288S mutant cDNA and incubated for 24 h. Next, cells were trypsinized and collected into tubes (Falcon) in 100 $\mu$L of 1× PBS (Gibco). Then, 1 mM ATP (Sigma) and YO-PRO1 (Invitrogen) were successively added. After samples had been diluted to 300 $\mu$L of 1× PBS and preincubated for 1−2 min in the dark, the fluorescence was measured using FACS Calibur (Becton Dickinson Biosciences instruments). Analyses were performed using BD CellQuest Pro Software (Becton Dickinson).

**Statistical Data Analysis.** Patch-clamp data were analyzed using the HEKA FitMaster and Origin 8.5 software (OriginLab). The significance of differences was tested with the paired two-tailed *t* test. Data presented as means ± the standard error of the mean (SEM) at the $*p < 0.05$ and $**p < 0.01$ level were accepted as significant. Best fits of data with a sigmoid function were compared with respective control fits using Origin 8.5.

## RESULTS

**Comparison of ATP Action on WT and F288S Rat P2X7 Receptors.** First, we compared the action of the natural agonist ATP on the temporal characteristics of WT and F288S rP2X7 receptors. ATP (1 mM) was applied either in short (2 s) pulses to minimize sensitization or in long pulses (20 s) to promote pore opening. When ATP was applied for 2 s, the most notable difference between the WT and mutant receptors was the longer time of current decay after the end of agonist application in the F288S receptor (Figure 1A). This decay (deactivation) that was well fitted with the monoexponential curve was ~3 times longer than in the WT receptor [for the WT, $\tau = 0.8 \pm 0.1$ s and $n = 29$, and for F288S, $\tau = 2.6 \pm 0.2$ s and $n = 24$; $p < 0.05$ (Figure 1A,B)], suggesting that the deactivation of the mutant receptor is a relatively slow process. The desensitization of the F288S receptor was also much slower [for the WT, $\tau_{DS} = 0.45 \pm 0.5$ s and $n = 7$, and for F288S, $\tau_{DS} = 3.09 \pm 1.35$ s and $n = 7$; $p < 0.05$ (Figure 1C)].

The dose−response curves for ATP did not show a significant difference in potency between WT and F288S [$EC_{50}$ values of 1.43 ± 0.22 mM ($n = 11$) and 1.27 ± 0.19 mM ($n = 10$), respectively]. However, the maximal responses to 3 and 5 mM ATP in the F288S mutant were lower ($p < 0.05$) than in the WT (Figure 1D).

As expected, a 20 s application of 1 mM ATP to the WT receptor induced an initial fast current growth followed by a slowly developing secondary peak (Figure 2A, left). The secondary peak that is known to be associated with

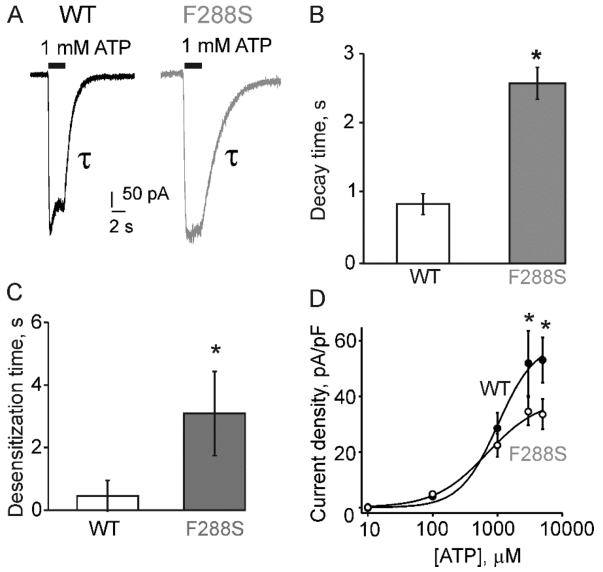


**Figure 1.** Membrane currents induced by the short-term application of ATP to the WT or F288S rat P2X7 receptors. (A) Representative currents elicited by 1 mM ATP (2 s applications) in the WT (black) and F288S mutant (gray) P2X7 receptors expressed in HEK cells. The black bar indicates the duration of agonist application. (B) Histograms showing the values of the monoexponential deactivation after the end of agonist application. Notice that deactivation was significantly ($p < 0.05$) slowed in the F288S mutant (2.6 ± 0.2 s; $n = 29$) in comparison to that in the WT (0.8 ± 0.1 s; $n = 24$). (C) Histograms showing the values of the monoexponential desensitization during agonist application. Notice that desensitization was significantly ($p < 0.05$) slowed in the F288S mutant (3.09 ± 1.35 s; $n = 7$) in comparison to that in the WT (0.45 ± 0.5 s; $n = 7$). (D) Dose−response curves obtained for the WT (●; $EC_{50} = 1.43 \pm 0.22$ mM; $n = 11$) and F288S mutant (○; $EC_{50} = 1.27 \pm 0.19$ mM; $n = 10$) activated by ATP. $*p < 0.05$.

sensitization was absent in the F288S receptor activated by 1 mM ATP (Figure 2A, right). However, like with short applications, the current decay after the end of agonist application was 3 times slower in F288S than in the WT receptor [for the WT, $\tau = 0.6 \pm 0.1$ s and $n = 5$, and for F288S, $\tau = 1.9 \pm 0.2$ s and $n = 6$; $p < 0.01$ (Figure 2A,B)]. The lack of a secondary peak in F288S suggested that this mutant has a lower probability of sensitization. To distinguish between these possibilities, we performed additional tests with higher ATP concentrations.

The application of 5 mM ATP for 20 s to the WT receptor induced a complex response with an initial current peak, and then the fast current decline followed by a slowly growing secondary peak (Figure 2C, left). A similar shape was observed by others[26,36] and was explained by initial desensitization after "normal" channel opening followed by sensitization. Notably, this higher concentration of ATP was enough to produce both phenomena (desensitization and pore opening) not only in the WT but also in the mutant F288S receptor (Figure 2C, right). However, in F288S, the amplitudes of the initial decline and of the secondary peak associated with the sensitization were smaller than in the WT receptor (Figure 2C, left), consistent with the lack of sensitization at lower ATP concentrations.

Interestingly, the development of sensitization in F288S was associated with an accelerated deactivation (Figure 2D). Thus, the large difference in current decay between the WT and F288S that we observed with short ATP applications (or with a


DOI: 10.1021/acs.biochem.7b00258
Biochemistry 2017, 56, 3394−3402

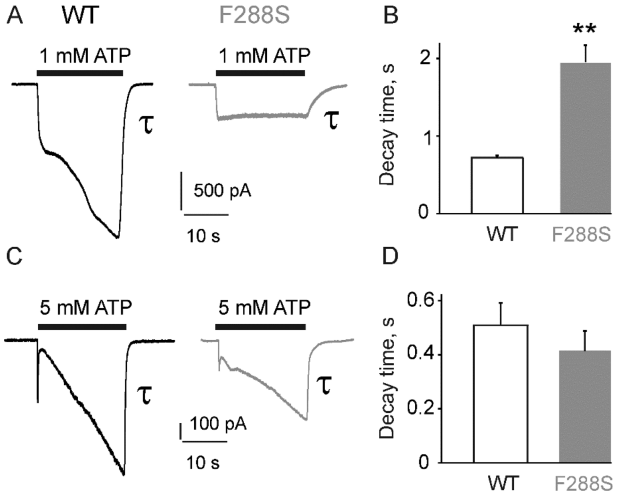


**Figure 2.** Membrane currents through the WT or F288S rat P2X7 receptors elicited by prolonged application of ATP. (A) Representative currents activated by 1 mM ATP (20 s application) in the WT (black) and F288S mutant (gray). Notice sensitization (secondary slow current growth) in the WT and lack of sensitization in F288S. (B) Histograms showing values of the monoexponential deactivation for the WT and F288S mutant. Notice that deactivation was significantly ($p < 0.01$) slower in the F288S mutant (1.9 ± 0.2 s, and $n = 6$; black column) than in the WT (0.7 ± 0.1 s, and $n = 6$; white column). (C) Representative currents activated by 5 mM ATP (20 s) in the WT (black) and F288S mutant (gray). (D) Histograms showing the values of monoexponential deactivation of the current generated by the WT and F288S mutant receptors. Notice that deactivation is approximately the same ($p > 0.05$) in the F288S mutant (0.4 ± 0.1 s; $n = 10$) and the WT (0.5 ± 0.1 s; $n = 8$). Data are expressed as means ± SEM. **$p <$ 0.01.

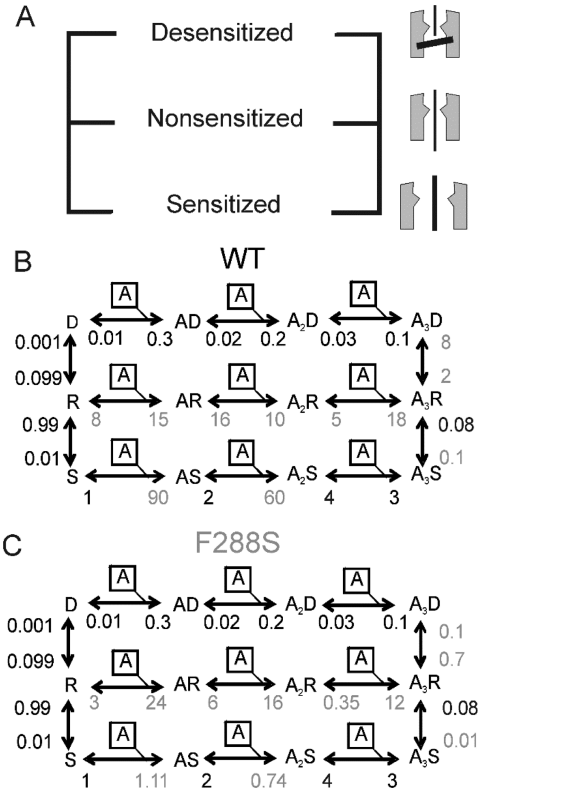


**Figure 3.** Kinetic model of the WT and F288S rat P2X7 receptor activated by ATP. (A) Principal structure of the model comprising three interactions of ATP with the receptor developing in parallel: activation of nonsensitized (middle) or sensitized states (bottom) and interactions of ATP with desensitized states (top). The cartoon on the right illustrates the conductive properties of all main conformations. Detailed kinetic scheme of the (B) WT P2X7 and (C) F288S mutant models (with rate constants for ATP). Notice that in each line the P2X7 receptor can bind from one to three ATP molecules. Double-bound ($A_2R$) and triple-bound ($A_3R$) nonsensitized receptors can open the "normal" state; however, double-bound ($A_2S$) and triple-bound ($A_3S$) sensitized receptors open 3 times more conductive pores, whereas desensitized states ($A_2D$ and $A_3D$) are always nonconductive. Values for rate constants are given in $mM^{-1}$ $s^{-1}$ (ATP binding steps) or $s^{-1}$ (all other steps). Rate constants different between panels B and C are colored gray. Other explanations are given in the text.

20 s application of 1 mM ATP) was lost with high ATP concentrations (for the WT, $\tau = 0.5 \pm 0.1$ s and $n = 8$, and for F288S, $\tau = 0.4 \pm 0.1$ s and $n = 10$; $p > 0.05$), suggesting rather different mechanisms of deactivation with and without sensitization.

Taken together, our data show the different kinetics of deactivation in the WT and F288S receptor and the promoting role of the wild-type amino acid F288 in maintaining the high probability of second peak development of the rP2X7 receptor.

**Kinetic Modeling of the WT P2X7 and F288S Mutant Activated by ATP.** The aims of our kinetic modeling were (i) to understand the role of sensitization in the deactivation mechanisms of the rP2X7 receptor, (ii) to determine what causes the decelerated current decay in the F288S mutant, (iii) to predict P2X7 receptor properties, and (iv) to explore receptor states normally "invisible" in the current recordings.

Using a kinetic model[26] we adopted for ATP action (the principal structure of the model is shown in Figure 3; for rate constants, see Figure 3B,C), we first reproduced the WT current during either 2 or 20 s application of 1 mM ATP. Figure 4A shows that the model reproduced the experimental current activated by a short application of ATP, whereas Figure 4C shows the first current peak, followed by the transient decline and secondary peak current (sensitization) activated by a 20 s application of 1 mM ATP. Next we reproduced currents generated in the F288S mutant by either 2 or 20 s applications of 1 mM ATP (panel B or D of Figure 4, respectively; rate constants are shown in Figure 3C). The slow current decay (deactivation) in the F288S mutant was simulated by reducing the speed of agonist unbinding (transition from $A_3R$ to R). The absence of transient initial decay and the lack of an $I_2$ peak in the F288S mutant receptors (Figure 4B,D) were simulated by decelerated transitions from nonsensitized open receptors ($A_3R$) to sensitized ($A_3S$) or desensitized ($A_3D$) states.

**Model Predictions and Experimental Validation.** Next, we checked if our model could reproduce the dependence of the current decay from the agonist concentration and the duration of its application for both the WT and F288S. Figure 5A shows that both in the model and under experimental conditions, the WT decay was independent of the concentration or duration of the ATP application [compare experimental decay (white columns) versus the model (black columns)]. Moreover, our model also simulated the unusual feature of F288S that gives a very different deactivation with and without sensitization (Figure 5B). Thus, the switch from slow (after a 0.2 or 2 s ATP pulse) to accelerated current decay (after 20 s with 5 mM ATP) for F288S can be explained by a prevailing receptor transition to the $A_3S$ state, whereas the recovery path ($A_3S \rightarrow \cdots S \rightarrow R$) has the same rate constants for the WT and F288S. Panels C and D of Figure 5 show the



DOI: 10.1021/acs.biochem.7b00258
Biochemistry 2017, 56, 3394−3402

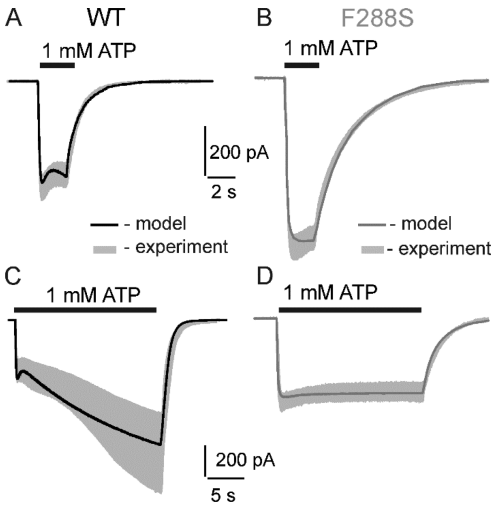


**Figure 4.** Validation of the model by comparison of experimental and simulated currents. Experimental (gray, mean ± SEM) and overlapping simulated (black) currents elicited by 1 mM ATP in the (A) WT and (B) F288S mutant during 2 s agonist applications. (C and D) The same for 20 s applications of 1 mM ATP. Notice that all model currents are within the experimental SEM.

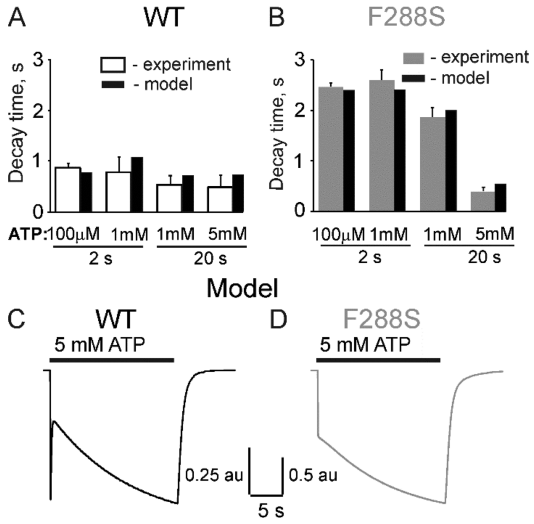


**Figure 5.** Experimental deactivation of the WT and F288S receptors in comparison with the model. Dependence of deactivation on the agonist concentration and the duration of ATP application to the (A) WT or (B) F288S receptor in experiment (white or gray columns) and in the model (black columns). Experimental data are expressed as the mean ± SEM. Model (C) WT or (D) F288S currents activated by a 20 s application of 5 mM ATP. Notice that all model currents are within the experimental SEM (au, arbitrary units).

simulated currents activated by a 20 s application of 5 mM ATP in the WT or F288S. Both model currents are within the experimental SEM.

**Characterization of rP2X7 Nonselective Pore Opening.** To quantify uptake of YO-PRO1 via the WT and F288S mutant, we used FACS. As a negative control, we used nontransfected HEK293 cells, which showed no change in YO-PRO1 uptake with or without ATP stimulation [2.5 ± 0.2% ($n$ = 9) vs 2.3 ± 0.3% ($n$ = 9)]. Long application (1−2 min) of 1 mM ATP followed by addition of YO-PRO1 was used to stimulate sensitization in WT and F288S receptors. We found an increased percentage of YO-PRO1 positive cells after application of ATP to WT rP2X7 compared to control values [15.3 ± 2.3% ($n$ = 8) vs 7.3 ± 0.4% ($n$ = 9); $p$ < 0.05 (Figure 6A,C)]. HEK cells expressing the F288S mutant did not show a

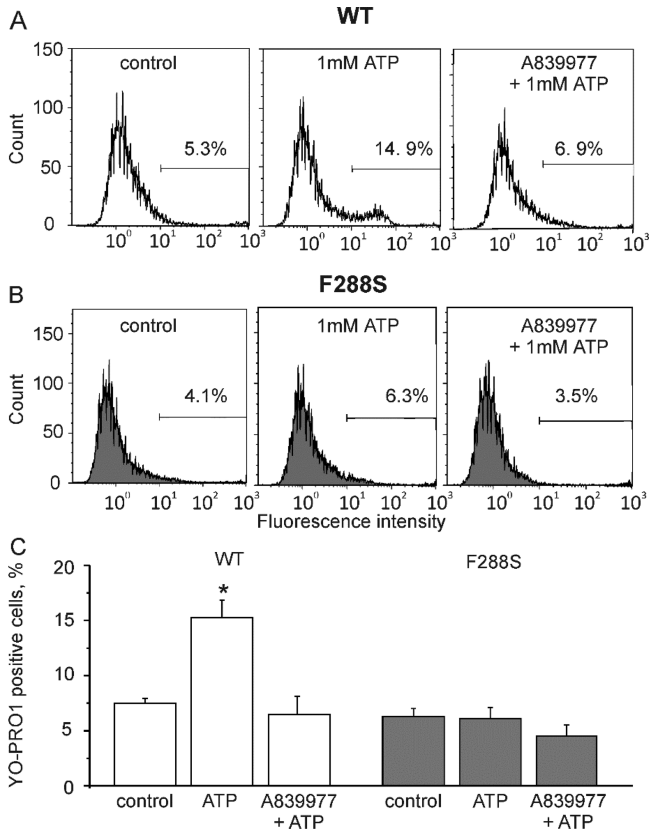


**Figure 6.** Evaluation of YO-PRO1 uptake by rP2X7 WT and F288S receptors expressed in a HEK293t culture. (A and B) Experimental histogram plots of control and 1 mM ATP-activated samples, respectively. For WT and F288S rP2X7 receptor subtypes: (A) transgenic rP2X7 WT and (B) recombinant rP2X7 F288S. (C) Histogram of statistical data for pore opening ($n$ = 9 for all except $n$ = 3 for the antagonist). *$p$ < 0.05.

significant difference in YO-PRO1 dye uptake after ATP application compared to control values [6.0 ± 0.3% ($n$ = 9) vs 6.5 ± 1.1% ($n$ = 9); $p$ < 0.05 (Figure 6B,C)]. The dye uptake in cells expressing WT rP2X7 was more than doubled after application of 1 mM ATP (Figure 6A,C). To test the role of P2X7 receptors in YO-PRO1 uptake, before ATP application, cells were preincubated with the selective P2X7 antagonist A839977 (10 μM) for 5 min. This antagonist prevented dye uptake in WT rP2X7 and the rP2X7 F288S mutant [6.4 ± 1.4% ($n$ = 3) and 4.9 ± 6.6% ($n$ = 3), respectively; $p$ > 0.05 (Figure 6C)].

Next, to test if, as seen for electrophysiological data, strong activation can promote dye uptake with the F288S rP2X7 mutant, we measured the YO-PRO1 fluorescence after application of 5 mM ATP. Figure 7 shows that, in cells expressing these mutant receptors, there was a significant uptake of YO-PRO1, analogous to that of the WT [for WT, 26.0 ± 1.5% vs 9.2 ± 1.5% in the control ($n$ = 6, and $p$ < 0.05); for F288S, 22.4 ± 3.5% vs 7.8 ± 0.8% in the control ($n$ = 7, and $p$ < 0.05)].



DOI: 10.1021/acs.biochem.7b00258
Biochemistry 2017, 56, 3394−3402

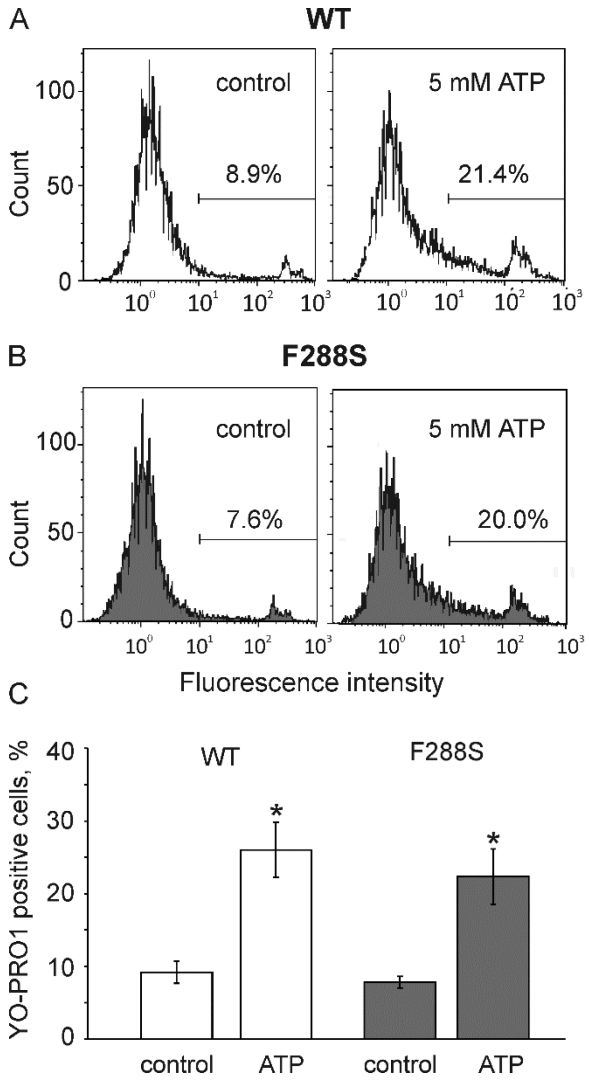


**Figure 7.** Uptake of YO-PRO1 by rP2X7 F288S and WT receptors. Representative histograms showing the action of 5 mM ATP on dye uptake in (A) WT and (B) F288S rP2X7 receptors. (C) Histograms of averaged data of YO-PRO1 uptake by WT and F288S rP2X7 receptors ($n$ = 6). *$p$ < 0.05.

These data together with the electrophysiology data confirm that the F288S mutant needs stronger stimulation than WT rP2X7 does to show significant YO-PRO1 uptake.

**Comparison of ATP Action on WT, Y288F, and Y288S hP2X7 Receptors.** In contrast to rP2X7, hP2X7 has a tyrosine at position 288. For this reason, we studied hP2X7 WT and two mutants: Y288F (rP2X7-like) and Y288S (288S mutant-like). We applied the same protocol for short applications (2 s) of ATP (1 mM) and found that hP2X7 mutant Y288F (rP2X7-like) has the fastest decay time, which was 2 times faster than that of WT hP2X7 or the Y288S mutant [$\tau$ = 0.45 ± 0.04 s ($n$ = 25) for the human Y288F mutant; $\tau$ = 0.74 ± 0.05 s ($n$ = 38) for the human WT; $\tau$ = 0.73 ± 0.05 s ($n$ = 25) for human Y288S and ($n$ = 34) rat WT (Figure 8B)]. hP2X7 WT and Y288S did not show difference in decay time (Figure 8). Nevertheless, tyrosine and serine are both polar amino acids, an important characteristic for the deactivation time of WT hP2X7 and the Y288S mutant. Our observation that phenylalanine at position 288 determines the fast deactivation of the WT receptor (Figures 4 and 5) is represented by a single mutation

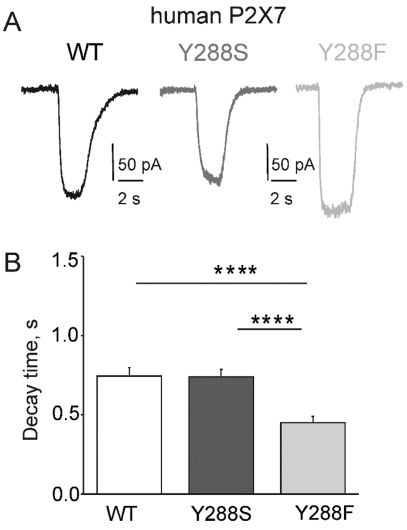


**Figure 8.** Membrane currents of the hP2X7 receptor and its mutants induced by the application of ATP. (A) Representative experimental currents elicited by 1 mM ATP (2 s applications) in the WT (black), Y288S mutant (dark gray), and Y288F rat-like mutant (light gray). (B) Histograms showing the values of the monoexponential deactivation after the end of agonist application. Notice that the rate of deactivation was significantly (***$p$ < 0.0001 vs WT and hY288S) increased in the Y288F mutant ($\tau$ = 0.45 ± 0.04 s; $n$ = 25) in comparison to those of the WT ($\tau$ = 0.74 ± 0.05 s; $n$ = 38) and Y288S ($\tau$ = 0.73 ± 0.05 s; $n$ = 25). The WT and Y288S did not show any significant difference. Data are expressed as the mean ± SEM.

in the hP2X7 receptor, the Y288F (rat-like) mutant. Comparison of panels A and B of Figure 1 and panels A and B of Figure 8 shows that the deactivation time of Y288F was even faster than that of WT rP2X7 [$\tau$ = 0.80 ± 0.11 s ($n$ = 29) for rat WT, and $\tau$ = 0.45 ± 0.04 s ($n$ = 25) for the human Y288F mutant].

**Molecular Modeling of the WT P2X7 Receptor and F288S Mutant.** To use a different approach for the investigation of the role of the F288 residue in the rP2X7 receptor, we constructed homology models of the ATP-bound form for both the WT receptor and the F288S mutant (Figure 9). This figure illustrates the location of the F288-containing left flipper loop in the receptor model. Figure 9A shows F288, located in the ATP binding pocket of the rP2X7 receptor. In the F288S mutant (Figure 9B), phenylalanine was replaced with serine. The side chain of S288 can potentially form a hydrogen bond with an ATP molecule, suggesting a direct role for the S288 residue in the binding of agonist molecules, as we showed earlier for S275 in the P2X3 receptor,[13] and as it was indeed subsequently confirmed by the X-ray structure.[7] This strongly corroborates the hypothesis of stabilization of nonsensitized states and the slow rate of ATP unbinding of the mutant rP2X7 receptor, proposed by the kinetic modeling approach.

## DISCUSSION

In this study, we provide a mechanistic explanation for the specific role of the residue at position 288 of the left flipper of the ectodomain of the rP2X7 receptor. The rationale behind the study was that all other P2X receptors have a serine at position 288 but rP2X7 possesses a phenylalanine there, which could underlie the specific properties of this receptor type. The left flipper itself is an important region for the normal function


DOI: 10.1021/acs.biochem.7b00258
Biochemistry 2017, 56, 3394−3402

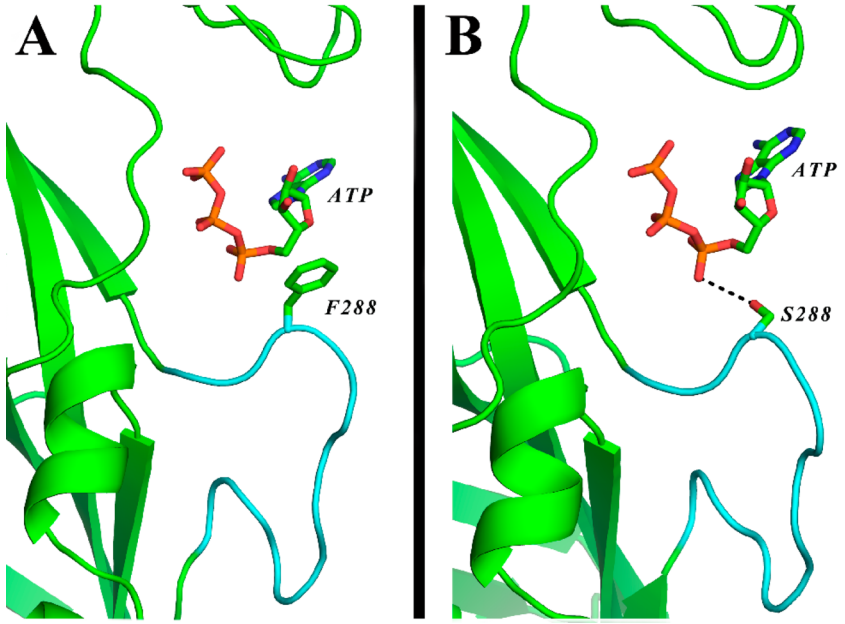


**Figure 9.** Homology model of the rat P2X7 receptor. Single P2X7 subunit with an ATP molecule bound. (A) WT binding pocket with an ATP molecule. (B) F288S mutant ATP binding pocket. The newly created H-bond between the ATP molecule and S288 side chain is indicated with a dashed line. The left flipper loop is colored cyan.

of all subtypes of P2X receptors.[1,7,14−16] We also previously reported that serine 275 (nomenclature of the P2X3 receptor), within the left flipper, which is in the position corresponding to F288 in rP2X7, is an important determinant of the specific properties of rP2X3 receptors: desensitization and exceptional sensitivity to extracellular calcium.[13] Thus, we suggested that residue S275 of rP2X3 plays an important role in the binding of ATP, and this interaction prevents fast dissociation of the agonist from the receptor binding cavity. The left flipper loop of rP2X7 has the same length as that of rP2X3 and rP2X4 but lacks the polar residue at position 288 (Figure 9A). From this, it was expected that replenishing S288F in the rP2X7 receptor would alter ATP−P2X7 interaction, most likely by helping to keep the ATP molecule in the binding pocket, thereby preventing fast agonist dissociation.[13] The newly created H-bond between residue S288 and the bound ATP molecule in the homology model (Figure 9B) strongly corroborates this proposal; phenylalanine, without a side chain, cannot interact in this manner with ATP, conferring these unique properties to rP2X7.

According to recent suggestions, in addition to the "normal" opening, the P2X7 receptor can transform into the sensitized state[26] that can be formally described as the progressive growth of the current during agonist application. We found that one of the key properties of the F288S mutant was the reduced probability of sensitization. Kinetic modeling not only suggested a simple explanation for the unusual phenotype of the F288S mutant but also allowed us to explore the complex relationships between different receptor states. As previously suggested by Khadra et al.,[26] there are three overlapping processes (opening of naïve, sensitized, and desensitized receptor states) triggered by binding of the agonist to the resting P2X7 receptors. We further developed a model of the P2X7 receptor activated by BzATP suggested by Khadra et al.[26] to simulate the action of the natural agonist ATP. Like in the model of Khadra et al.,[26] there are three lines of receptor transformation induced by agonists that we call the "non-sensitized" state (normal opening) and sensitized (associated with $I_2$) and desensitized (inactive, closed ion channel) receptor states (Figure 3). As discussed by Khadra et al.,[26] the occupancy of one or two ATP binding sites of naïve receptors favors a slow transition to desensitized states, whereas occupancy of the third binding site favors a transition to sensitized and/or dilated states. Notably, two recent papers mainly based on P2X2, P2X3, P2X4, and P2X5 receptor studies challenged the possibility of progressive pore dilation in P2X receptors.[29,30] They suggested that these channels are immediately permeable to both small ions and organic molecules, excluding YO-PRO1, which only slowly accumulates in cells. In this way, our results with fluorescent dye uptake (obtained at one time point after a relatively long exposure to YO-PRO1) do not contradict the data of Harkat et al.[30] Moreover, these authors did not completely exclude the possibility of pore dilation but proposed that this needs some external regulatory elements. Finally, Harkat et al.[30] did not use high (≥1 mM) concentrations of ATP that are needed to observe desensitization, a phenomenon that nature (ionic redistribution or intrinsic receptor mechanism) has not solved. It is clear that more experiments are needed to clarify further P2X7 receptor-specific properties such as sensitization and desensitization.

One of our key findings, however, is that the mutation of F288 to S largely slowed receptor deactivation. A similar slow deactivation was detected recently in the P2X7 receptor co-activated with ultraviolet light,[37] resulting in slow agonist unbinding. Likewise, we previously proposed slow agonist unbinding as a reason for slow deactivation of the P2X3 receptor.[38] We therefore used this mechanism in our kinetic modeling to provide a mechanistic explanation for slow current decay, one of the key properties of the F288S mutant. The changes in decay rate were simulated by decelerated agonist unbinding ($A_3R \rightarrow \cdots R$ transitions), and the absence of the $I_2$ peak could be best explained by deceleration of the transition from a nonsensitized open to sensitized state ($A_3R \rightarrow \cdots A$



DOI: 10.1021/acs.biochem.7b00258
*Biochemistry* 2017, 56, 3394−3402

transitions). When the F288S mutated P2X7 receptor is activated by 1 mM ATP, there is a "balance" between sensitization and desensitization of nonsensitized receptor states, which is provided by slowing substantially the binding of ATP to sensitized receptors (compare panels B and C of Figure 3).

Thus, in addition to its contribution to sensitization, we also show that the natural Phe in the left flipper of the rP2X7 receptor determines the rate of deactivation. Figures 4 and 5 show that the kinetic model simulates well experimental traces. It can be argued that F288S does not prevent sensitization but only lowers the probability of these transitions. The global result is that a single F288S mutation can stabilize all nonsensitized states as represented in our FACS experiments [not allowing sensitization or developing simultaneous desensitization (Figure 6B,C)]. Thus, in WT rP2X7, amino acid F288 provides fast unbinding for nonsensitized states and also fast transitions into sensitized or desensitized states.

Data for YO-PRO1 uptake suggest that higher (5 mM) concentrations of ATP can allow the F288S rP2X7 mutant to enter the sensitization state, in agreement with our electrophysiological results. This is rather in favor of a view that electrophysiologically observed current growth and a significant increase in the rate of YO-PRO1 uptake are linked to the same molecular conformational change in the P2X7 receptor.[39] However, the exact pathway providing YO-PRO1 uptake is still unclear. It could be a slow penetration via the ion channel of the P2X receptor[30] or through associated proteins such as pannexins.[40] However, the low level of expression of endogenous pannexins in HEK cells argues against the latter.[41]

Moreover, mutation Y288F in the hP2X7 receptor provides further evidence that the F amino acid at position 288 can significantly decrease the decay time (Figure 8A,B) and suggests faster agonist unbinding. Replacement of polar Y with polar S at position 288 of hP2X7 did not affect the decay time and suggests similar rates in ATP unbinding times (Figure 8B).

Importantly, our kinetic model, like the recent works of Li et al.[29] and Harkat et al.,[30] suggests potentially parallel activation of not only normal but also sensitized and desensitized states (Figure 3). Also, our kinetic model suggests that the sensitization can contribute even to the short duration responses (without the visible secondary peak traditionally attributable to sensitization).

The physiological role of P2X7 receptors in immunological responses has been widely discussed.[23,42] Basic mechanisms of P2X7 receptor functioning revealed in this project may help improve our understanding of the functional properties of ATP-gated receptors and the design new drugs for neurodegenerative diseases or for chronic pain conditions where the role of P2X7 receptors is well-established.[43]

## AUTHOR INFORMATION


### Corresponding Author

*A. I. Virtanen Institute, University of Eastern Finland, FI-70211, P.O. Box 1627, Neulaniementie 2, Kuopio, Finland. Telephone: +358 40 355 3665. Fax: +358 17 163 030. E-mail: rashid.giniatullin@uef.fi.

### ORCID

Nataliia Novosolova: 0000-0003-1248-165X

Rashid Giniatullin: 0000-0002-1580-6280


### Author Contributions

R.G. and A.S. participated in research design and general supervision of the project. Y.I., N.N., G.B., D.F., and A.T. conducted experiments. Y.I., N.N., and A.S. performed data analysis. K.K. created molecular models of the receptors. A.S. developed and described the kinetic model. N.N., Y.I., G.B., A.S., K.K. R.G., and D.F. drafted the manuscript. Y.I., G.B., N.N., A.S., K.K., and R.G. edited and revised the manuscript. Y.I., G.B., N.N., A.S., K.K., D.F., R.G., and A.T. approved the final manuscript. Y.I. and N.N. made equal contributions for first authorship. A.S. and R.G. made equal contributions for last authorship.


### Funding

The study was supported by the Finnish Academy (Grant 277442). A.S. was supported by the Program of the Presidium of the Russian Academy of Sciences. R.G. was supported by the Program of Competitive Growth of Kazan Federal University.


### Notes

The authors declare no competing financial interest.

## ACKNOWLEDGMENTS


The authors are grateful to H. Zemkova, Claverol J. Viladoms, and Y. Peter for providing the F288S, Y288S, and Y288F mutants. Also, the authors thank Watson for critical reading of the manuscript and JVC for help with figure preparation.


## ABBREVIATIONS

WT, wild type; rP2X7, rat P2X7; hP2X7, human P2X7; pP2X7, giant panda P2X7; BzATP, benzoylbenzoyl-ATP.

## REFERENCES


(1) Burnstock, G. (2007) Physiology and pathophysiology of purinergic neurotransmission. *Physiol. Rev. 87*, 659−797.

(2) Kawate, T., Michel, J. C., Birdsong, W. T., and Gouaux, E. (2009) Crystal structure of the ATP-gated P2X4 ion channel in the closed state. *Nature 460*, 592−598.

(3) Duckwitz, W., Hausmann, R., Aschrafi, A., and Schmalzing, G. (2006) P2X5 subunit assembly requires scaffolding by the second transmembrane domain and a conserved aspartate. *J. Biol. Chem. 281*, 39561−39572.

(4) Mittal, R., Grati, M., Sedlacek, M., Yuan, F., Chang, Q., Yan, D., Lin, X., Kachar, B., Farooq, A., Chapagain, P., Zhang, Y., and Liu, X. Z. (2016) Characterization of ATPase activity of P2RX2 cation channel. *Front. Physiol. 7*, 186.

(5) Hattori, M., and Gouaux, E. (2012) Molecular mechanism of ATP binding and ion channel activation in P2X receptors. *Nature 485*, 207−212.

(6) Karasawa, A., and Kawate, T. (2016) Structural basis for subtype-specific inhibition of the P2X7 receptor. *eLife 5*, e22153.

(7) Mansoor, S. E., Lü, W., Oosterheert, W., Shekhar, M., Tajkhorshid, E., and Gouaux, E. (2016) X-ray structures define human P2X3 receptor gating cycle and antagonist action. *Nature 538*, 66−71.

(8) Kasuya, G., Fujiwara, Y., Tsukamoto, H., Morinaga, S., Ryu, S., Touhara, K., Ishitani, R., Furutani, Y., Hattori, M., and Nureki, O. (2017) Structural insights into the nucleotide base specificity of P2X receptors. *Sci. Rep. 7*, 45208.

(9) Kasuya, G., Fujiwara, Y., Takemoto, M., Dohmae, N., Nakada-Nakura, Y., Ishitani, R., Hattori, M., and Nureki, O. (2016) Structural insights into divalent cation modulations of ATP-gated P2X receptor channels. *Cell Rep. 14*, 932−944.

(10) Khakh, B. S., and North, R. A. (2006) P2X receptors as cell-surface ATP sensors in health and disease. *Nature 442*, 527−532.

(11) Khakh, B. S., and North, R. A. (2012) Neuromodulation by extracellular ATP and P2X receptors in the CNS. *Neuron 76*, 51−69.




DOI: 10.1021/acs.biochem.7b00258
*Biochemistry* 2017, 56, 3394−3402

(12) Burnstock, G., Nistri, A., Khakh, B. S., and Giniatullin, R. (2014) ATP-gated P2X receptors in health and disease. *Front. Cell. Neurosci. 8*, 204.
(13) Petrenko, N., Khafizov, K., Tvrdonova, V., Skorinkin, A., and Giniatullin, R. (2011) Role of the ectodomain serine 275 in shaping the binding pocket of the ATP-gated P2X3 receptor. *Biochemistry 50*, 8427−8436.
(14) Adriouch, S., Scheuplein, F., Bähring, R., Seman, M., Boyer, O., Koch-Nolte, F., and Haag, F. (2009) Characterisation of the R276A gain-of-function mutation in the ectodomain of murine P2X7. *Purinergic Signalling 5*, 151−161.
(15) Kowalski, M., Hausmann, R., Dopychai, A., Grohmann, M., Franke, H., Nieber, K., Schmalzing, G., Illes, P., and Riedel, T. (2014) Conformational flexibility of the agonist binding jaw of the human P2X3 receptor is a prerequisite for channel opening. *Br. J. Pharmacol. 171*, 5093−5112.
(16) Zhao, W.-S., Wang, J., Ma, X.-J., Yang, Y., Liu, Y., Huang, L.-D., Fan, Y.-Z., Cheng, X.-Y., Chen, H.-Z., Wang, R., and Yu, Y. (2014) Relative motions between left flipper and dorsal fin domains favour P2X4 receptor activation. *Nat. Commun. 5*, 4189.
(17) Khakh, B. S., Bao, X. R., Labarca, C., and Lester, H. A. (1999) Neuronal P2X transmitter-gated cation channels change their ion selectivity in seconds. *Nat. Neurosci. 2*, 322−330.
(18) Virginio, C., MacKenzie, A., Rassendren, F. A., North, R. A., and Surprenant, A. (1999) Pore dilation of neuronal P2X receptor channels. *Nat. Neurosci. 2*, 315−321.
(19) Collo, G., Neidhart, S., Kawashima, E., Kosco-Vilbois, M., North, R. A., and Buell, G. (1997) Tissue distribution of the P2X7 receptor. *Neuropharmacology 36*, 1277−1283.
(20) Rassendren, F., Buell, G. N., Virginio, C., Collo, G., North, R. A., and Surprenant, A. (1997) The permeabilizing ATP receptor, P2X7. Cloning and expression of a human cDNA. *J. Biol. Chem. 272*, 5482−5486.
(21) Di Virgilio, F., Ceruti, S., Bramanti, P., and Abbracchio, M. P. (2009) Purinergic signalling in inflammation of the central nervous system. *Trends Neurosci. 32*, 79−87.
(22) Chessell, I. P., Hatcher, J. P., Bountra, C., Michel, A. D., Hughes, J. P., Green, P., Egerton, J., Murfin, M., Richardson, J., Peck, W. L., Grahames, C. B. A., Casula, M. A., Yiangou, Y., Birch, R., Anand, P., and Buell, G. N. (2005) Disruption of the P2X7 purinoceptor gene abolishes chronic inflammatory and neuropathic pain. *Pain 114*, 386−396.
(23) Skaper, S. D., Debetto, P., and Giusti, P. (2010) The P2X7 purinergic receptor: from physiology to neurological disorders. *FASEB J. 24*, 337−345.
(24) Solle, M., Labasi, J., Perregaux, D. G., Stam, E., Petrushova, N., Koller, B. H., Griffiths, R. J., and Gabel, C. A. (2001) Altered cytokine production in mice lacking P2X7 receptors. *J. Biol. Chem. 276*, 125−132.
(25) Weisman, G. A., Camden, J. M., Peterson, T. S., Ajit, D., Woods, L. T., and Erb, L. (2012) P2 receptors for extracellular nucleotides in the central nervous system: role of P2X7 and $P2Y_2$ receptor interactions in neuroinflammation. *Mol. Neurobiol. 46*, 96−113.
(26) Khadra, A., Tomić, M., Yan, Z., Zemkova, H., Sherman, A., and Stojilkovic, S. S. (2013) Dual gating mechanism and function of P2X7 receptor channels. *Biophys. J. 104*, 2612−2621.
(27) Giniatullin, R., Nistri, A., and Yakel, J. (2005) Desensitization of nicotinic ACh receptors: shaping cholinergic signaling. *Trends Neurosci. 28*, 371−378.
(28) Katz, B., and Thesleff, S. (1957) A study of the desensitization produced by acetylcholine at the motor end-plate. *J. Physiol. 138*, 63−80.
(29) Li, M., Toombes, G. E. S., Silberberg, S. D., and Swartz, K. J. (2015) Physical basis of apparent pore dilation of ATP-activated P2X receptor channels. *Nat. Neurosci. 18*, 1577−1583.
(30) Harkat, M., Peverini, L., Cerdan, A. H., Dunning, K., Beudez, J., Martz, A., Calimet, N., Specht, A., Cecchini, M., Chataigneau, T., and Grutter, T. (2017) On the permeation of large organic cations through the pore of ATP-gated P2X receptors. *Proc. Natl. Acad. Sci. U. S. A. 114*, E3786−E3795.
(31) Webb, B., and Sali, A. (2016) Comparative protein structure modeling using MODELLER. *Current Protocols in Bioinformatics 54*, 5.6.1−5.6.37.
(32) Stamm, M., Staritzbichler, R., Khafizov, K., and Forrest, L. R. (2013) Alignment of helical membrane protein sequences using AlignMe. *PLoS One 8*, e57731.
(33) Edgar, R. C. (2004) Muscle: multiple sequence alignment with high accuracy and high throughput. *Nucleic Acids Res. 32*, 1792−1797.
(34) Waterhouse, A. M., Procter, J. B., Martin, D. M. A., Clamp, M., and Barton, G. J. (2009) Jalview Version 2–a multiple sequence alignment editor and analysis workbench. *Bioinformatics 25*, 1189−1191.
(35) Michel, A. D., Chessell, I. P., and Humphrey, P. P. A. (1999) Ionic effects on human recombinant P2X7 receptor function. *Naunyn-Schmiedeberg's Arch. Pharmacol. 359*, 102−109.
(36) Yan, Z., Li, S., Liang, Z., Tomić, M., and Stojilkovic, S. S. (2008) The P2X7 receptor channel pore dilates under physiological ion conditions. *J. Gen. Physiol. 132*, 563−573.
(37) Browne, L. E., and North, R. A. (2013) P2X receptor intermediate activation states have altered nucleotide selectivity. *J. Neurosci. 33*, 14801−14808.
(38) Jindrichova, M., Khafizov, K., Skorinkin, A., Fayuk, D., Bart, G., Zemkova, H., and Giniatullin, R. (2011) Highly conserved tyrosine 37 stabilizes desensitized states and restricts calcium permeability of ATP-gated P2X3 receptor. *J. Neurochem. 119*, 676−685.
(39) Virginio, C., MacKenzie, A., North, R. A., and Surprenant, A. (1999) Kinetics of cell lysis, dye uptake and permeability changes in cells expressing the rat P2X7 receptor. *J. Physiol. 519*, 335−346.
(40) Pelegrin, P., and Surprenant, A. (2007) Pannexin-1 couples to maitotoxin- and nigericin-induced interleukin-1$\beta$ release through a dye uptake-independent pathway. *J. Biol. Chem. 282*, 2386−2394.
(41) Browne, L. E., Compan, V., Bragg, L., and North, R. A. (2013) P2X7 receptor channels allow direct permeation of nanometer-sized dyes. *J. Neurosci. 33*, 3557−3566.
(42) Alves, L. A., Bezerra, R. J. S., Faria, R. X., Ferreira, L. G. B., and da Silva Frutuoso, V. (2013) Physiological roles and potential therapeutic applications of the P2X7 receptor in inflammation and pain. *Molecules 18*, 10953−10972.
(43) Inoue, K., and Tsuda, M. (2012) Purinergic systems, neuropathic pain and the role of microglia. *Exp. Neurol. 234*, 293−301.


DOI: 10.1021/acs.biochem.7b00258
*Biochemistry* 2017, 56, 3394−3402